An Approach to the Structure Determination of Larger Proteins Using Triple Resonance NMR Experiments in Conjunction with Random Fractional Deuteration

Daniel Nietlispach,[⊥] Robin T. Clowes,[#] R. William Broadhurst,[#] Yutaka Ito,[#,†] James Keeler,[⊥] Mark Kelly,[§] Jennifer Ashurst,[§] Hartmut Oschkinat,[§] Peter J. Domaille,[‡] and Ernest D. Laue*[,#]

Contribution from the Cambridge Centre for Molecular Recognition, Department of Biochemistry, University of Cambridge, Tennis Court Road, Cambridge CB2 1QW, U.K., the Department of Chemistry, University of Cambridge, Lensfield Road, Cambridge CB2 1EW, U.K., the European Molecular Biology Laboratory, Meyerhofstrasse 1, 69012 Heidelberg, Germany, and the Du Pont Merck Pharmaceutical Company, Box 80328, Wilmington, Delaware 19880-0328

Received July 5, 1995[⊗]

Abstract: A combination of simulation and experiment is used to demonstrate that the sensitivity of a family of 3D/4D NMR experiments used to assign resonances and to obtain structural restraints in proteins is improved by *partial* random deuteration; the improvement increases as the correlation time of the protein becomes longer. The results suggest that deuteration at a level of ∼50% optimizes the sensitivity of experiments which are used to assign sidechain ^{1}H and ^{13}C resonances by correlating them with the resonances from backbone nuclei. In addition, this level of deuteration is also a good compromise for recording NOESY experiments. Using this approach, it should be possible to determine structures of larger proteins.

Introduction

The development of heteronuclear triple resonance NMR experiments, in conjunction with essentially complete enrichment with ^{13}C and ^{15}N, has dramatically increased the scope of the NMR method for structural studies of biological macromolecules.[1,2] For example, structure determination of proteins of 150−200 amino acid residues is now becoming a matter of routine, whereas a few years ago studies using ^{1}H NMR methods were limited to proteins of less than 100 residues or so. With the exception of very favorable cases, however, studies of larger proteins, *e.g.* of 200−300 amino acid residues, are still difficult in large part due to rapid relaxation which limits the transfer of magnetization between coupled nuclei.

Many years ago it was shown that fractional deuteration of proteins improves the resolution and sensitivity of ^{1}H NMR experiments.[3−6] The origin of this effect is that the substitution of D for ^{1}H reduces the rate of dipole−dipole relaxation of the observed protons simply because the gyromagnetic ratio of deuterium is 6.5 times smaller than that of proton. The result is that the lines are sharper and so more intense. Subsequently it was shown that similar sensitivity improvements could be obtained in ^{15}N-separated experiments.[6−9] More recently, it has been demonstrated that the sensitivity of certain heteronuclear triple-resonance NMR experiments is improved by *complete* deuteration of all but the exchangeable H_N protons.[10−13] In these experiments the sensitivity improvement results from two effects: first, all the nuclei, and in particular the ^{13}C, relax more slowly thus allowing more magnetization to be transferred between *J*-coupled nuclei;[10,12,14] second, the slower relaxation of $^{1}H_N$ nuclei results in sharper, more intense lines in the observed spectrum.[15] In addition, the slower relaxation of ^{13}C makes it possible to extend the length of the evolution period so as to obtain higher resolution in the indirect dimensions.[11,12]

In this paper we show that the sensitivity of a class of three- and four-dimensional NMR experiments used to assign *sidechain* ^{1}H and ^{13}C resonances of proteins is improved by *partial* random deuteration. In these triple-resonance experiments the observed signal is derived from magnetization originating on a *sidechain proton*. Complete deuteration is, therefore, not appropriate. However, although fractional deuteration decreases the number of sidechain protons, and thus the size of the original magnetization, it also increases the relaxation times of the ^{13}C nuclei thus resulting in more efficient *J* transfer between nuclei and

* To whom correspondence should be addressed.
[#] Department of Biochemistry, University of Cambridge.
[⊥] Department of Chemistry, University of Cambridge.
[†] On leave from the Laboratory of Cellular and Molecular Biology, Institute of Physical and Chemical Research (RIKEN), 2−1 Hirosawa, Wako, Saitama 351−01, Japan.
[§] European Molecular Biology Laboratory.
[‡] Du Pont Merck Pharmaceutical Company.
[⊗] Abstract published in *Advance ACS Abstracts,* December 15, 1995.

(1) Bax, A.; Grzesiek, S. *Acc. Chem. Res.* **1993**, *26*, 131−138.
(2) Clore, G. M.; Gronenborn, A. *Science* **1991**, *252*, 795−796.
(3) Crepsi, H. L.; Rosenberg, R. M.; Katz, J. J. *Science* **1968**, *161*, 795−796.
(4) Markley, J. L.; Potter, I.; Jardetzky, O. *Science* **1968**, *161*, 1249−1251.
(5) LeMaster, D. M.; Richards, F. M. *Biochemistry* **1988**, *27*, 142−150.
(6) LeMaster, D. M. *Q. Rev. Biophys.* **1990**, *23*, 133−174.
(7) Torchia, D. A.; Sparks, S. W.; Bax, A. *J. Am. Chem. Soc.* **1988**, *110*, 2320−2321.
(8) Arrowsmith, C. H.; Pachter, R.; Altman, R. B.; Iyer, S. B.; Jardetzky, O. *Biochemistry* **1990**, *29*, 6332−6341.
(9) Reisman, J.; Jariel-Encontre, I.; Hsu, V. L.; Parell, J.; Geiduschek, E. P.; Kearns, D. R. *J. Am. Chem. Soc.* **1991**, *113*, 2787−2789.
(10) Grzesiek, S.; Anglister, J.; Ren, H.; Bax, A. *J. Am. Chem. Soc.* **1993**, *115*, 4369−4370.
(11) Yamazaki, T.; Lee, W.; Revington, M.; Mattiello, D. L.; Dahlquist, F. W.; Arrowsmith, C. H.; Kay, L. E. *J. Am. Chem. Soc.* **1994**, *116*, 6464−6465.
(12) Yamazaki, T.; Lee, W.; Arrowsmith, C. H.; Muhandiram, D. R.; Kay, L. E. *J. Am. Chem. Soc.* **1994**, *116*, 11655−11666.
(13) Farmer, B. T.; Venters, R. A. *J. Am. Chem. Soc.* **1995**, *117*, 4187−4188.
(14) Kushlan, D. M.; LeMaster, D. M. *J. Biomol. NMR* **1993**, *3*, 701−708.
(15) Markus, M. A.; Dayie, K. T.; Matsudaira, P.; Wagner, G. *J. Magn. Reson. Ser. A* **1994**, *105*, 192−195.

0002-7863/96/1518-0407$12.00/0

so giving stronger signals. The optimum level for fractional deuteration is determined by the balance between these two opposing effects; we show by calculation and experiment that this optimum level is around 50%. The sensitivity improvement resulting from this level of deuteration increases as the overall correlation time, τ_c, of the protein becomes larger: for $\tau_c \sim 18$ ns a sensitivity improvement by a factor of between 1.5 and 2.5 when compared to the protonated protein has been observed. We also consider the effect that deuteration has on the sensitivity of three- and four-dimensional $^{13}C/^{15}N$-separated NOESY spectra and show that there is no one level of deuteration which optimizes the intensity of all the different types of cross peaks in the spectrum. However, it is shown that a 50% deuterated sample gives very usable spectra. These results suggest that a single 50% deuterated sample can be used to advantage for both assignment and the measurement of NOE contacts. The sensitivity improvement of the crucial sidechain experiments should help make it possible to increase the size of protein whose structure can be studied by NMR.

Experimental Section

Uniformly ^{13}C- and ^{15}N-labeled SH3 domain proteins (from chicken brain alpha spectrin) with random fractional deuteration levels of 0, 50, and 75% were isolated from *E. coli* strain BL21 (DE3)/pET.SH3.[16] For production of the labeled SH3 domains, cells were grown in 1 L of M9 minimal medium[17] supplemented with 1 g of $^{15}NH_4Cl$ and 4 g/L of either $^{13}C/^{15}N$ plant cell hydrolysate or [50−75% ^2H, 100% ^{13}C,^{15}N] algal hydrolysate (EMBL labeling facility, EMBL, Heidelberg, Germany). For the preparation of the [50% ^2H, 100% ^{13}C,^{15}N] SH3 domains, cells were adapted to growth in D_2O as follows. Cells were first grown in LB medium[17] with 50% D_2O (v/v) at 37 °C to an apparent optical density at 600 nm of 1.0. For the preparation of the [75% ^2H, 100% ^{13}C,^{15}N] SH3 domain, cells adapted to 50% D_2O were used to inoculate LB medium with 75% D_2O and grown to the same density. For the large-scale production of [50−75% ^2H, 100% ^{13}C,^{15}N] SH3 domains, 1-L cultures of M9 minimal medium supplemented with 1 g of $^{15}NH_4Cl$ and 4 g of either [50% ^2H, 100% ^{13}C,^{15}N] or [75% ^2H, 100% ^{13}C,^{15}N] algal hydrolysate, in the corresponding ratio of H_2O/D_2O, were inoculated with adapted cells. Cell growth rates were slower in D_2O; cultures containing 0, 50, and 75% (v/v) D_2O had doubling times of 0.7, 1.3, and 1.6 per hour, respectively. The proteins were purified as described previously[16] and concentrated to ∼1 mM in 30% (v/v) glycerol and 1 mM NaN_3 at pH 3.5.

NMR experiments were recorded on a three-channel Bruker AMX 600 spectrometer equipped with a 5 mm $^1H/^{13}C/^{15}N$ triple-resonance probe head, pulsed field gradients, and a home built fourth channel used for ^2H decoupling. The lock receiver was gated off during either ^2H decoupling or the application of pulsed field gradients which required some small modifications to our spectrometer. The HBCB/HACANNH spectra were acquired, in 7 h (at 8 and 12 ns) and in 28 h (at 18 ns), with 43 (t_1) and 512 (t_2) complex points to give final acquisition times of 4.3 (t_1) and 63.5 (t_2) ms. The HBCB/HACA(CO)NNH and HCC(CO)NNH spectra were acquired, in 14 and 11 h, respectively, with 39 (t_1) and 512 (t_2) complex points to give final acquisition times of 3.9 (t_1) and 63.5 (t_2) ms. The ^{13}C- and ^{15}N-separated NOESY spectra were acquired with 128 (t_1) and 512 (t_2) complex points to give final acquisition times of 15.9 (t_1) and 63.5 (t_2) ms, respectively. All spectra were recorded using repetition rates optimized for the protonated protein; slight increases in the sensitivity of the spectra of the deuterated proteins are to be expected using somewhat longer relaxation delays.

Results and Discussion

We first consider the method by which the relaxation rate constants of partially deuterated proteins can be calculated and then discuss the way in which the relaxation of different nuclei is affected by deuteration. The calculated relaxation rate constants are then used to predict the effect of deuteration on the sensitivity of various sidechain and separated NOE experiments and these predictions are compared with experiment. We have focused on the HBCB/HACANNH experiment,[18−20] in which both intra- and interresidue correlations are observed, and on the HBCB/HACA(CO)NNH experiment,[19,21] in which only the interresidue correlations are observed, as in our experience the combination of these experiments provides a quick and simple approach to obtaining assignments. We have also considered the HCC(CO)NNH experiment,[22−24] in which all the aliphatic ^1H and ^{13}C sidechain resonances are correlated with the backbone ^{15}N and ^1H_N nuclei, as, sensitivity permitting, this is also particularly useful for obtaining more complete sidechain assignments.[25]

Calculation of Relaxation Rate Constants in Randomly Fractionally Deuterated Proteins. In order to be able to calculate the amount of magnetization which is left at the end of a pulse sequence a knowledge of the relaxation rate constants relevant to each period in the sequence is required. For the present work, the way in which these rates vary with deuteration level is also needed. However, in a partially deuterated protein sample we cannot talk of the relaxation rate constant of a particular nucleus. This is because the sample consists of an ensemble of different isotopomers in each of which the nuclei of interest will have a different relaxation rate constant. The observed relaxation behavior of the magnetization from the whole sample will be the sum of the relaxation behavior of the magnetization from each isotopomer, the contribution from each weighted by its population. Therefore, to calculate the outcome of an experiment on a partially deuterated sample it would be necessary to consider each isotopomer *individually*. The calculation of the contribution made by each isotopomer to the observed magnetization would be rather laborious, although by no means impossible.

For the calculations presented below we have adopted a simpler approach which will be shown to be a good approximation to the complete calculation. This approach is based on computing an *average rate constant*, determined by taking a population weighted average of the rate constants for each isotopomer. In general the resulting average rate constant will *not* represent the observed decay of magnetization from the whole sample. This decay is in principle a sum of many different decay curves and there is no reason to assume that the overall decay can be represented by a single rate constant. However, there are two cases where this overall decay is well represented by the average rate constant.

The first of these is when the spread of relaxation rate constants for different isotopomers is small compared to their absolute values. In this case the magnetization from different isotopomers decays at rather similar rates, so the assumption that the total magnetization decays at a rate determined by a mean rate constant is a good approximation to the actual decay. An example of this is the relaxation of ^{13}C in a $^{13}C^1H$ or ^{15}N in an $^{15}N^1H$ group. In these cases the relaxation of the heteronucleus is dominated by the attached proton; substituting

(16) Musacchio, A.; Noble, M.; Pauptit, R.; Wierenga, R.; Saraste, M. *Nature* **1992**, *359*, 851−854.
(17) Maniatis, T.; Fritsch, E. F.; Sambrook, J. *Molecular Cloning: A Laboratory Manual*; Cold Spring Harbor: Cold Spring Harbor Laboratory, 1986.
(18) Grzesiek, S.; Bax, A. *J. Magn. Reson.* **1992**, *99*, 201−207.
(19) Grzesiek, S.; Bax, A. *J. Biomol. NMR* **1993**, *3*, 185−204.
(20) Wang, A. C.; Lodi, P. J.; Qin, J.; Vuister, G. W.; Gronenborn, A. M.; Clore, G. M. *J. Magn. Reson. B* **1994**, *105*, 196−198.
(21) Grzesiek, S.; Bax, A. *J. Am. Chem. Soc.* **1992**, *114*, 6291−6293.
(22) Montelione, G. T.; Lyons, B. A.; Emerson, S. D.; Tashiro, M. *J. Am. Chem. Soc.* **1992**, *114*, 10974−10975.
(23) Logan, T. M.; Olejniczak, E. T.; Xu, R. X.; Fesik, S. W. *FEBS Lett.* **1992**, *314*, 413−418.
(24) Clowes, R. T.; Boucher, W.; Hardman, C. H.; Domaille, P. J.; Laue, E. D. *J. Biomol. NMR* **1993**, *3*, 349−354.
(25) Clowes, R. T.; Crawford, A.; Raine, A. R. C.; Smith, B. O.; Laue, E. D. *Curr. Opin. Biotech.* **1995**, *6*, 81−88.

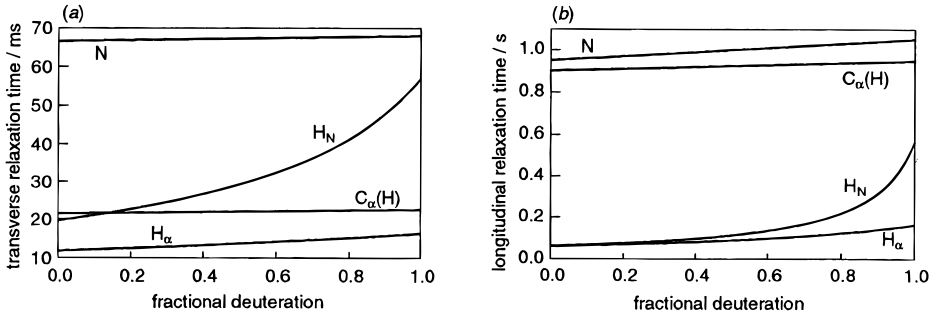

Figure 1. *Average* relaxation times (as defined in the text) computed for different nuclei in a protein as a function of deuteration level: (a) transverse and (b) longitudinal relaxation times. The overall correlation time was taken as 12 ns and the field strength was 14.1 T; see text for further details of how these relaxation times were calculated.

deuterium for all the other protons in the protein changes the relaxation rate constant by less than 2%. The case of ^{13}CD is less clear-cut as, when compared to the contribution from the attached D, the contribution to the relaxation of ^{13}C by other protons is more significant; we have, nevertheless, used an average rate. Note that although it is quite valid to use an average rate for the ^{13}C relaxation in ^{13}CH or ^{13}CD it would not be appropriate to average these two values together, as they differ markedly. In analyzing an experiment these two contributions must be considered separately.

The second case where an average relaxation rate constant may be used is when the decay of magnetization is computed in the initial rate limit. In this limit the decay of the magnetization from each isotopomer is linear, and the sum of such decays is also linear with a slope determined by the average rate. An example of where this case is applicable is in considering the decay of transverse ^1H_N and $^1H_{\alpha/\beta}$ magnetizations during INEPT transfer delays which are sufficiently short that the decay can be considered to be in the initial rate.

These average relaxation rate constants can be computed without explicit averaging over an ensemble of isotopomers. The average relaxation rate constant, $R_{\rm av}^{{\rm CH}_n{\rm D}_m}$, for a ^{13}C with n and m directly attached protons and deuterons, respectively, can be computed from

$$R_{\rm av}^{{\rm CH}_n{\rm D}_m} = R_{\rm CSA} + R_{\rm X}^{\rm C} + nR_{\rm CH}^{\rm C} + mR_{\rm CD}^{\rm C} + R_{{\rm H}_{\rm N}}^{\rm C} + (1-\alpha)R_{\rm H}^{\rm C} + \alpha R_{\rm D}^{\rm C} \quad (1)$$

where α is the fractional deuteration level, $R_{\rm CSA}$ is the contribution due to the chemical shift anisotropy of the ^{13}C, $R_{\rm X}^{\rm C}$ is the contribution due to dipole−dipole (DD) interaction with other ^{13}C and ^{15}N nuclei, $R_{\rm CH}^{\rm C}$ and $R_{\rm CD}^{\rm C}$ are the contributions due to the DD interaction between the ^{13}C and the directly attached proton or deuteron respectively, and $R_{{\rm H}_{\rm N}}^{\rm C}$ is the contribution due to the DD interaction between the ^{13}C and the H_N protons (the exchangeable hydrogens are not deuterated). $R_{\rm H}^{\rm C}$ is the sum of the contributions due to DD interactions between ^{13}C and all the other hydrogen atoms in a protein molecule which is entirely protonated. Likewise $R_{\rm D}^{\rm C}$ is the sum of all contributions due to DD interactions between ^{13}C and all the other hydrogen atoms in a molecule which is entirely deuterated. The H_N protons are excluded from the calculation of $R_{\rm H}^{\rm C}$ and $R_{\rm D}^{\rm C}$; these protons are never replaced by deuterium and their contribution to relaxation is given by the term $R_{{\rm H}_{\rm N}}^{\rm C}$. The simple way in which the level of deuteration appears in eq 1 is a consequence of the fact that the dipolar interactions are all considered to be pairwise and additive. The relaxation rate constant for ^{15}N in an ^{15}NH pair can be computed using an expression analogous to eq 1.

The relaxation rate constants for H_N, H_α, and H_β protons are computed in a similar way:

$$R_{\rm av}^{\rm H} = R_{\rm X}^{\rm H} + R_{{\rm H}_{\rm N}}^{\rm H} + (1-\alpha)R_{\rm H}^{\rm H} + \alpha R_{\rm D}^{\rm H} \quad (2)$$

where $R_{\rm X}^{\rm H}$ is the sum of all the contributions due to DD interaction with ^{13}C and ^{15}N, and $R_{{\rm H}_{\rm N}}^{\rm H}$ is the sum of all contributions due to DD interactions between the proton of interest and all of the H_N protons. As before, $R_{\rm H}^{\rm H}$ is the sum of the contributions due to DD interactions between the proton of interest and all of the remaining hydrogens in a protonated protein, $R_{\rm D}^{\rm H}$ is the same, but for a protein in which the remaining hydrogens are deuterated.

A knowledge of the positions of all NMR active nuclei is needed in order to compute $R_{{\rm H}_{\rm N}}^{\rm H}$, $R_{\rm D}^{\rm C}$, *etc.* For the simulations presented here the coordinates from the X-ray structure of the SH3 domain from chicken brain alpha spectrin were used.[16] The various relaxation rate constants were computed using the well-known formulae[26] in which the spectral density function was of the form suggested by Lipari and Szabo.[27,28] The internal correlation times were set as 50 ps and the order parameter, S^2, was set to 0.86, values which are representative of residues in well-structured parts of the protein. The CSA tensor for ^{15}N was assumed to be axially symmetric with an anisotropy of −160 ppm;[29] the $^{13}C_\alpha$ CSA tensor was likewise assumed to be axially symmetric with an anisotropy of 25 ppm.[30]

The average relaxation rate constants computed using the approach outlined in eqs 1 and 2 were compared with values derived from calculations in which an explicit average of rate constants, for 1500 different structures, randomly deuterated to a particular level, was calculated; the rate constants computed by both methods were in good agreement. In addition, we also found that both methods gave little variation in the values of the rate constants for the same nuclei in different residues.

Figure 1 shows calculated *average* relaxation times, as a function of deuteration level, for different nuclei in the protein; the correlation time has been set to 12 ns and it is assumed that the H_N are always protonated. (In the following discussion the proton and deuteron will be used to refer specifically to the isotopes ^{1}H and ^{2}H; an atom which may be either ^{1}H or ^{2}H will be referred to as a hydrogen atom.) The transverse relaxation times of both ^1H_N and $^1H_\alpha$ increase with increasing deuteration although the effect is greater for ^1H_N. The relaxation times of ^{15}N barely change as they are dominated by the DD interaction with the attached proton which is not exchanged for deuterium. Also shown is the relaxation data for a $^{13}C_\alpha$ in which it is

(26) Peng, J. W.; Wagner, G. *Methods in Enzymology*; James, T. L.; Oppenheimer, N., Eds.; Academic Press: San Diego, 1994; Vol. 239C.
(27) Lipari, G.; Szabo, A. *J. Am. Chem. Soc.* **1982**, *104*, 4546−4559.
(28) Lipari, G.; Szabo, A. *J. Am. Chem. Soc.* **1982**, *104*, 4559−4570.
(29) Hiyama, Y.; Niu, C.; Silverton, J. V.; Bavoso, A.; Torchia, D. A. *J. Am. Chem. Soc.* **1988**, *110*, 2378−2383.
(30) Palmer, A. G.; Rance, M.; Wright, P. E. *J. Am. Chem. Soc.* **1991**, *113*, 4371−4380.
(31) Marion, D.; Kay, L. E.; Sparks, S. W.; Torchia, D. A.; Bax, A. *J. Am. Chem. Soc.* **1989**, *111*, 1515−1517.

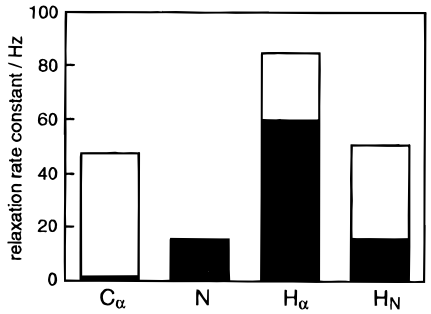

Figure 2. Bar chart showing how the transverse relaxation rate constants for various nuclei are partitioned between two contributions: the *fixed part* (solid bar) and the *variable part* (open bar). The terms *fixed* and *variable* are defined in the text. Broadly speaking, the contribution from the variable part can be eliminated by deuteration of the protein. The data are presented for a fully protonated protein and all other parameters are the same as those used to compute the data shown in Figure 1.

assumed that the attached H_α is always a proton. As with the ^{15}NH the relaxation is dominated by the attached proton and deuteration of the rest of the molecule has little effect.

Figure 2 visualizes the contributions to the total relaxation rate constant for different nuclei in the protein. For the present discussion it is useful to separate the relaxation into two contributions: a *fixed part* and a *variable part*. The variable part is due to interaction with hydrogens which may be exchanged for deuterium; the fixed part is due to all other interactions which are unaffected by deuteration, for example, CSA and DD interaction with ^1H_N. This bar chart shows directly the extent to which deuteration can alter the relaxation of different nuclei; broadly speaking, complete deuteration of the non-exchangeable hydrogens will remove the variable part of the relaxation rate (the open bar). The chart also shows how deuteration reduces the relaxation rate constant of $^{13}C_\alpha$ by a factor of ~10; this dramatic change is almost entirely due to the effect of replacing the attached proton by deuterium. In a $^{13}CH_2$ group replacing one of the protons by deuterium reduces the relaxation rate constant by a factor of around 2. It is on these reductions of the ^{13}C relaxation rate constant that much of the advantage of partial deuteration rests. Finally, it must be remembered that the sensitivity of an experiment will also be affected by the dilution effect that deuteration has on the protons, something which is not represented in either Figure 1 or 2.

The HBCB/HACANNH Experiment. This experiment is designed to correlate the shifts of sidechain ^1H and ^{13}C nuclei with those of the backbone;[18−20] the pulse sequence is shown in Figure 3a. Magnetization starts from H_β, is transferred first to C_β, then to C_α, and then via the relatively small $^1J_{NC\alpha}$ (11 Hz) and $^2J_{NC\alpha}$ (7 Hz) couplings to N. A final transfer step to H_N is followed by observation of this proton. The amount of magnetization which is transferred from H_β to H_N can be computed provided that the relevant couplings and relaxation rate constants are known. In addition, when considering a partially deuterated sample the population of proton or deuterium at the various sites also needs to be considered.

In the analysis of the HBCB/HACANNH experiment four different arrangements of proton and deuterium at the α and β positions need to be considered:

$C_\beta H_2-C_\alpha H$	$C_\beta HD-C_\alpha H$	$C_\beta H_2-C_\alpha D$	$C_\beta HD-C_\alpha D$
I	**II**	**III**	**IV**

The populations of these fragments are $(1-\alpha)^3$, $2\times(1-\alpha)^2\times\alpha$, $(1-\alpha)^2\times\alpha$, and $2\times(1-\alpha)\times\alpha^2$, respectively, where α is the fractional deuteration level. For each of these fragments the average relaxation rates are determined as described above and these are used to compute the amount of magnetization that is observable on H_N at the end of the pulse sequence. The total amount of observable magnetization is found by first multiplying the contribution from each fragment by its population and then summing these weighted contributions over all fragments. The calculation is then repeated for different levels of deuteration and finally the results are normalized by dividing by the amount of magnetization expected from the fully protonated sample; this calculation gives the *relative transfer efficiency* as a function of deuteration level. As explained above, it is not appropriate to average the relaxation rates of fragments **I**−**IV** as these rates differ markedly.

During many of the delays in the pulse sequence in-phase and anti-phase magnetization evolve into one another. The relaxation rate constants of these two types of magnetization are generally not the same and this has to be allowed for when calculating how much magnetization is lost during a delay. One approach is to subdivide the delay into very small steps and then allow couplings and relaxation to act sequentially during these small delays. For sufficiently small delays this approximation turns out to be an excellent one; it is, however, a rather laborious calculation. In order to make our calculations simpler we have assumed that during delays in which there is significant interchange of in- and anti-phase magnetization the decay can be modeled by a simple average of the rate constants of the in-phase and anti-phase magnetization. The results of calculations made with and without this approximation have been compared and it was found that the relative transfer efficiency plot is not perturbed significantly by the approximation.

A plot of the calculated relative transfer efficiency for the HBCB/HACANNH sequence is shown in Figure 4a for three different overall correlation times. This plot shows that the relative transfer efficiency is a maximum at a deuteration level of around 50%, and that as the correlation time increases the advantage to be gained from deuteration also increases. For the longest correlation time, 18 ns, the signal from the 50% deuterated sample is predicted to be 2.4 times stronger than that from the fully protonated sample; the sensitivity improvement is certainly significant.

It seems clear that most of this enhancement can be attributed to the much slower C_α relaxation in fragments **III** and **IV**. The slower relaxation rate of this carbon is particularly important in determining the sensitivity of the experiment as the small size of the $N-C_\alpha$ coupling requires the inclusion of a delay of some 22 ms during which this coupling evolves into anti-phase. As ^{13}C transverse relaxation times for slowly tumbling proteins can be rather short, typically 14 ms for $\tau_c = 18$ ns, there is a very significant loss of magnetization during this dephasing delay. In fragments **III** and **IV** the substitution of the H_α by D increases the ^{13}C transverse relaxation time by a factor of ~10 leading to the loss of much less magnetization. As the level of deuteration increases the advantage due to slower relaxation is eventually outweighed by the loss of H_β protons. In the case of a 50% deuterated protein with a correlation time of 18 ns the calculated contributions of the fragments **I**−**IV** to the finally observed magnetization are 4%, 16%, 17%, and 63%, respectively; these can be compared with their populations which are 12.5%, 25%, 12.5%, and 25%, respectively. As expected, **III** and **IV** together are the major contributors as they have much slower $^{13}C_\alpha$ relaxation than **I** and **II**; **IV** contributes more than **III** on account of the slower relaxation of both the $^{13}C_\beta$ and the remaining H_β and also on account of its higher population.

The HBCB/HACANNH sequence also results in the transfer of magnetization from H_α to H_N; Figure 4a also shows the

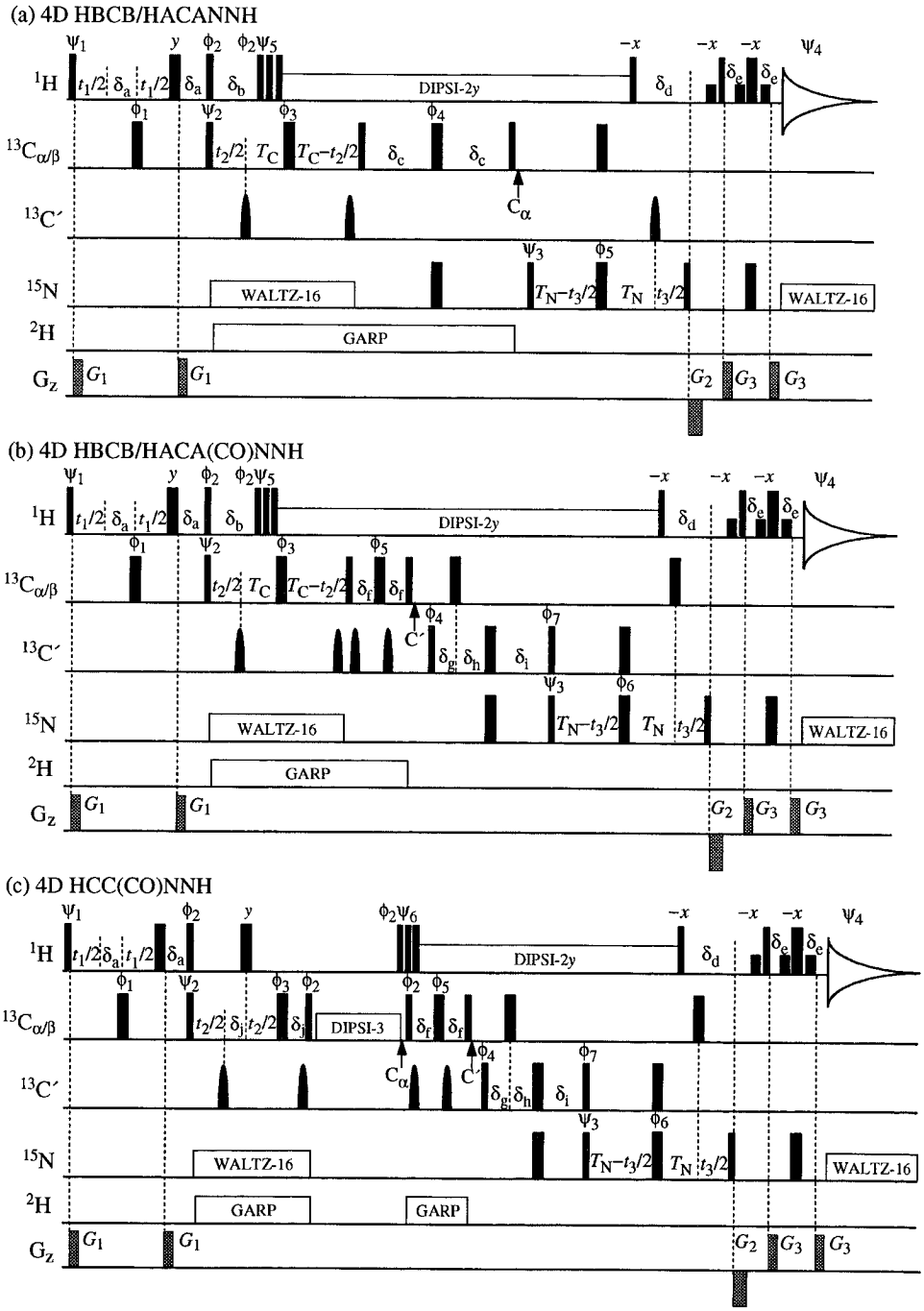

Figure 3. Pulse sequences for (a) the 4D HBCB/HACANNH, (b) the 4D HBCB/HACA(CO)NNH, and (c) the 4D HCC(CO)NNH experiments; corresponding pathways of magnetization transfer are shown in Figure 4. Narrow boxes represent 90° radio-frequency (RF) pulses, wider boxes represent 180° RF pulses, and cross hatched boxes (G_1−G_3) represent gradient pulses. The water selective 90° ^{1}H RF pulses (half height boxes) were of 1.2 ms duration. The 180° sinebell-shaped pulses are phase modulated and of duration 201.6 μs.[21] ^{1}H and ^{15}N RF pulses were applied with field strengths of 32.5 and 5.1 kHz, respectively, except during the periods of DIPSI-2 or WALTZ-16 decoupling where the RF field strength was reduced to either 5.3 or 1.0 kHz, respectively. $^{13}C_{\alpha/\beta}$ and $^{13}C_\alpha$ pulses were applied with field strengths of 5.1 and 4.6 kHz (for 90° pulses) or 11.4 and 10.4 kHz (for 180° pulses) for $^{13}C_{\alpha/\beta}$ and $^{13}C_\alpha$, respectively. $^{13}C'$ pulses were applied with a field strength of 4.6 kHz. The carrier was set to 46, 57, and 174 ppm respectively for $^{13}C_{\alpha/\beta}$, $^{13}C_\alpha$, and $^{13}C'$; the frequency is switched from $^{13}C_{\alpha/\beta}$ to $^{13}C_\alpha$ or $^{13}C'$ where indicated. ^{2}H GARP decoupling was applied using a 1.0-kHz field with the carrier at 4.5 ppm. Gradient pulses were applied with durations and strengths as follows: $G_1 = 0.4$ ms (20 G cm^{-1}); $G_2 = 2.0$ ms (50 G cm^{-1}); and $G_3 = 0.4$ ms (35 G cm^{-1}). Typical values for the delays are $\delta_a = 1.5$ ms, $\delta_b = 2.0$ ms, $\delta_c = 11.0$ ms, $\delta_d = 5.4$ ms, $\delta_e = 2.25$ ms, $\delta_f = 3.7$ ms, $\delta_g = 4.5$ ms, $\delta_h = 7.9$ ms, $\delta_i = 12.4$ ms, $\delta_j = 0.9$ ms, $T_C = 3.1$ ms; for the HBCB/HACANNH experiment $T_N = 11.2$ ms while for the HBCB/HACA(CO)NNH and HCC(CO)NNH experiments $T_N = 12.0$ ms. The following phase cycling was employed: $\phi_1 = x, -x$; $\phi_2 = y, -y$; $\phi_3 = 8(x), 8(y), 8(-x), 8(-y)$; $\phi_4 = 2(x), 2(-x)$; $\phi_5 = 4(x), 4(-x)$; $\phi_6 = 8(x), 8(-x)$; $\phi_7 = 53°$; and $\psi_1 = \psi_2 = x$. $\psi_3 = 2(x), 2(-x)$ and $\psi_4 = 2(x, -x, -x, x), 2(-x, x, x, -x)$ for the HBCB/HACANNH experiment and $4(x), 4(-x)$ and $x, -x, -x, x, 2(-x, x, x, -x)$, $x, -x, -x, x$ for the HBCB/HACA(CO)NNH and HCC(CO)NNH experiments. Unless indicated otherwise all pulses were of phase x. Quadrature detection in F_1, F_2, and F_3 is achieved by altering ψ_1, ψ_2, and ψ_3 in a States-TPPI, States, and States-TPPI[40] manner, respectively, to shift the axial peaks in F_1 and F_3 to the edge of the spectrum. ψ_5 and ψ_6 are phase cycled $-x, -y, x, y$ and $-x, y, x, -y$ in concert with ψ_1 so that the water magnetization remains on the $+z$ axis at the end of the pulse sequence.[41−44]

relative transfer efficiency for this process. In contrast to the case of transfer from H_β, increasing the level of deuteration always results in a reduced transfer efficiency. The reason for this is that only fragments **I** and **II** contribute to the observed signal; the fragments in which the $^{13}C_\alpha$ is relaxing more slowly, **III** and **IV**, do not contribute to the spectrum as they have no

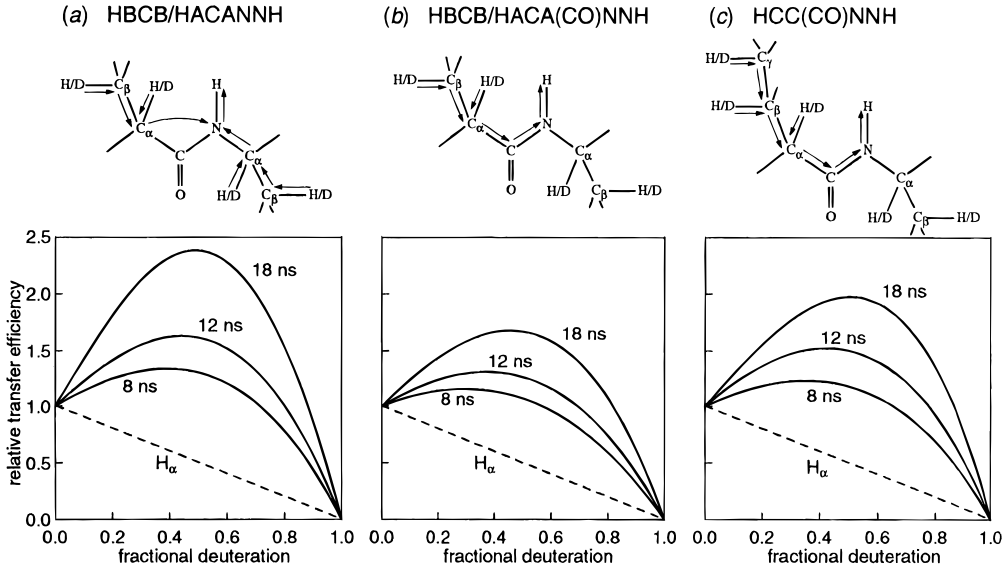

Figure 4. Plots of the *relative transfer efficiency* (defined in the text) as a function of deuteration level for various different sidechain experiments. In each plot the solid lines show the relative transfer efficiency for magnetization originating on the H_β protons for three different correlation times, 8, 12, and 18 ns. The dashed line shows the relative transfer efficiency for magnetization originating on the H_α protons for a correlation time of 12 ns; the form of the transfer function for H_α is hardly affected by variation in the correlation time in the range 8−18 ns. Plots a, b, and c are computed for the 4D HBCB/HACANNH, the 4D HBCB/HACA(CO)NNH, and the 4D HCC(CO)NNH experiments, respectively. The pathways for magnetization transfer corresponding to each experiment are shown above each plot.

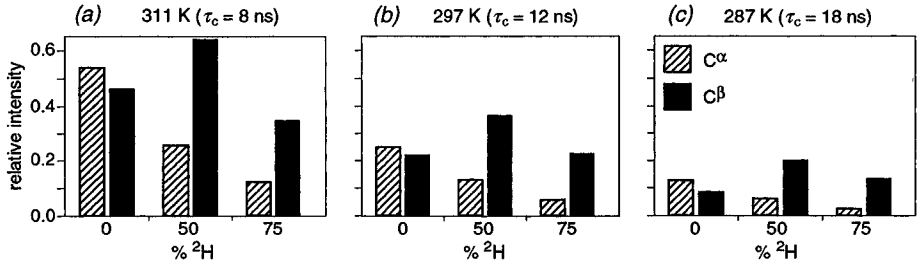

Figure 5. Bar charts illustrating the relative intensity (by volume integration) of the sum of either all the $^{13}C_\alpha$ cross peaks (hatched bars) or all the $^{13}C_\beta$ cross peaks (filled bars) in 2D $^1H_N-^{13}C$ correlation spectra recorded using the 4D HBCB/HACANNH experiment whose pulse sequence is shown in Figure 3a. The intensities are relative to the sum of all the ^{13}C cross-peaks in the spectrum of the fully protonated sample recorded at 311 K. Data are shown for three different temperatures of 311, 297, and 287 K, histograms a, b, and c, respectively, and for three different protein samples, of identical concentration, randomly fractionally deuterated to levels of either 0%, 50%, or 75%. The overall correlation times of the samples were determined from ^{15}N relaxation measurements to be 8, 12, and 18 ns at 311, 297, and 287 K, respectively.

H_α proton. Deuteration thus offers no advantage for the observation of correlations between the H_α and H_N nuclei.

In order to verify the results of these calculations we have recorded spectra from three samples of an SH3 domain deuterated to levels of 0%, 50%, and 75%; the protein concentration was the same in each. The samples were prepared in a water/glycerol mixture (30% glycerol by volume). By varying the temperature we were able to obtain overall correlation times in the range 8−18 ns. Thus, although the SH3 domain is itself a small protein (62 residues) the sample conditions enable us to use it to model the behavior of several much larger proteins with long correlation times.

Two-dimensional $^1H_N-^{13}C$ spectra were recorded using the pulse sequence of Figure 3a on each sample and at three different temperatures, giving correlation times of 8, 12, or 18 ns. (These correlation times were estimated by analyzing ^{15}N T_1 and T_2 data using the approach of Lipari and Szabo.[27,28]) The volumes of the cross peaks were analyzed and a summary of the results is given in Figure 5. As expected, at each correlation time, the relative intensity of the cross peaks originating from H_α is reduced to 0.5 and 0.75 of those from the fully protonated sample in the spectra of the 50% and 75% deuterated proteins, respectively. However, consistent with the simulations, the relative intensity of the cross peaks originating from H_β is greatest in the spectra of the 50% labeled protein, with increases by factors of 1.38, 1.67, and 2.30 as compared to the fully protonated sample, at correlation times of 8, 12, and 18 ns, respectively. To illustrate further the results, the spectra recorded at a correlation time of 12 ns are shown in Figure 6. A significantly higher proportion of cross peaks to C_β can be observed in the spectrum of the 50% deuterated protein (>85% at 18 ns; these numbers were estimated by analyzing cross peaks that are resolved in the 2D $^1H-^{13}C$ correlation spectra) than in the spectra of either the fully protonated or the 75% deuterated sample. In contrast, the intensity of the cross peaks to C_α decrease as the level of deuteration increases.

The HBCB/HACA(CO)NNH and HCC(CO)NNH Experiments. These experiments are closely related to the HBCB/HACANNH experiment in that the magnetization is transferred via the rapidly relaxing $^{13}C_\alpha$. We thus expect that partial deuteration will give significant improvements in the sensitivity of the experiments, and these expectations are born out by the plots of the relative transfer efficiency shown in Figure 4, parts b and c. As before the most efficient transfer is obtained for a deuteration level of around 50%, and the greatest improvement is predicted for the most slowly tumbling protein. Again, as in the HBCB/HACANNH experiment, deuteration results in less efficient transfer from the H_α protons. The HBCB/HACA(CO)-NNH experiment shows a smaller improvement than does the

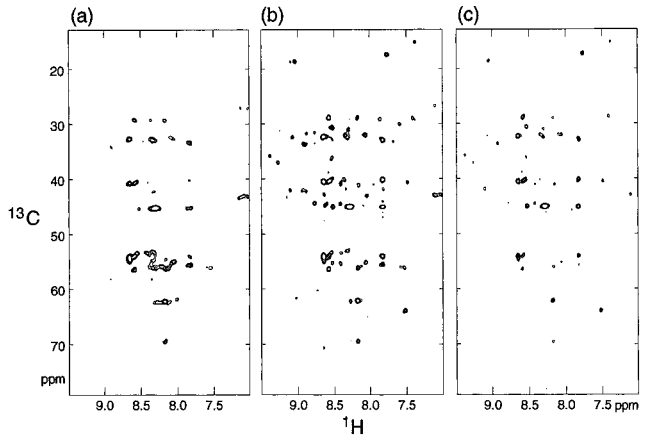

Figure 6. Two-dimensional $^{1}H_N$ - ^{13}C spectra recorded using the 4D HBCB/HACANNH pulse sequence of Figure 3 (a) at 297 K (equivalent to a correlation time of 12 ns). In (a), (b) and (c) the spectra of the protonated, the 50% labelled and the 75% labelled samples, respectively, are shown.

HBCB/HACANNH experiment as the magnetization spends less time on C_α in the former than in the latter experiment.

The pulse sequences for the HBCB/HACA(CO)NNH[19,21] and HCC(CO)NNH[22−24] experiments are shown in Figure 3, parts b and c, respectively. Having shown with the HBCB/HACANNH experiment that our simulations predict the experimentally observed variation in signal with deuteration level, we simply confirmed the sensitivity advantage in these latter experiments by recording spectra for the fully protonated and 50% deuterated proteins. Figure 7 shows the comparison for the HBCB/HACA(CO)NNH experiment for a correlation time of 18 ns; the signal intensity from the 50% deuterated sample is increased, on average, by a factor of 1.7 when compared to the fully protonated sample; this is in good agreement with the theoretical predictions. Figure 7 also shows a comparison for the HCC(CO)NNH experiment for a correlation time of 12 ns; again in line with the theoretical predictions the signals from the 50% deuterated sample are, on average, 1.4 times stronger than those from the fully protonated sample. It is also apparent that more correlations to C_γ are visible in the spectrum from the 50% deuterated sample. At a correlation time of 18 ns the signals from the 50% deuterated sample are, on average, 1.8 times stronger than those from the fully protonated sample (data not shown). Although at this correlation time the absolute sensitivity of the HCC(CO)NNH experiment is rather less than for the HBCB/HACA(CO)NNH experiment we observed >95% (estimated by analyzing cross peaks that are resolved in the 2D $^{1}H-^{13}C$ correlation spectra) of the expected cross peaks in both spectra.

NOESY Experiments. From the foregoing discussion it is clear that a deuteration level of ∼50% optimizes the sensitivity of experiments designed to correlate sidechain resonances with those of the backbone nuclei. We now turn to the question of the effect of deuteration on three- and four-dimensional separated NOESY spectra.

As is shown in Figure 1a and Figure 2 the transverse relaxation times of the H_N protons increase markedly as the protein is deuterated. The resulting line narrowing will cause an increase in peak height and so NOE cross peaks between H_N protons are thus expected to increase in intensity as the level of deuteration increases. The intensity of a cross peak between an H_N and an H_α will behave rather differently; two factors are involved. First, increasing deuteration will simply dilute the H_α proton, reducing the cross-peak intensity. Second, the transverse relaxation time of the H_α increases as the protein is deuterated, but this effect is not as marked as it is for the H_N proton (see Figures 1a and 2). For a cross peak between non-exchangeable protons, increasing the level of deuteration has an even stronger diluting effect than for a cross peak involving just one non-exchangeable proton. For the latter two types of cross peaks it is not immediately obvious what the balance between the dilution and relaxation effects will be.

Figure 8 shows the calculated relative peak height expected for different types of NOESY cross peaks plotted as a function of deuteration level. These heights are calculated for, in the case of the H_N-H_N and $H_\alpha-H_N$ cross peaks, three-dimensional ^{15}N separated spectra, and in the case of $H_\alpha-H_\alpha$ and $H_\beta-H_\alpha$ cross peaks, three-dimensional ^{13}C separated spectra. This plot takes into account the effect on peak height of relaxation of protons and ^{13}C or ^{15}N in all three dimensions; the influence of changing relaxation rates on the efficiency of the INEPT transfer steps is also included. However, no account is taken of the influence of the mixing time on the peak height (vide infra). In addition, the effect that removing proton−proton couplings has on the peak height is not included in this plot. It is expected that these effects will favor higher deuteration levels. As expected, the intensity of the H_N-H_N cross peaks simply rises with increasing level of deuteration. The H_N-H_α cross-peak intensity varies little up to a deuteration level of around 50% and then begins to fall off; at first the dilution effect is compensated for by the more favorable relaxation of the remaining protons, but at higher deuteration levels the dilution

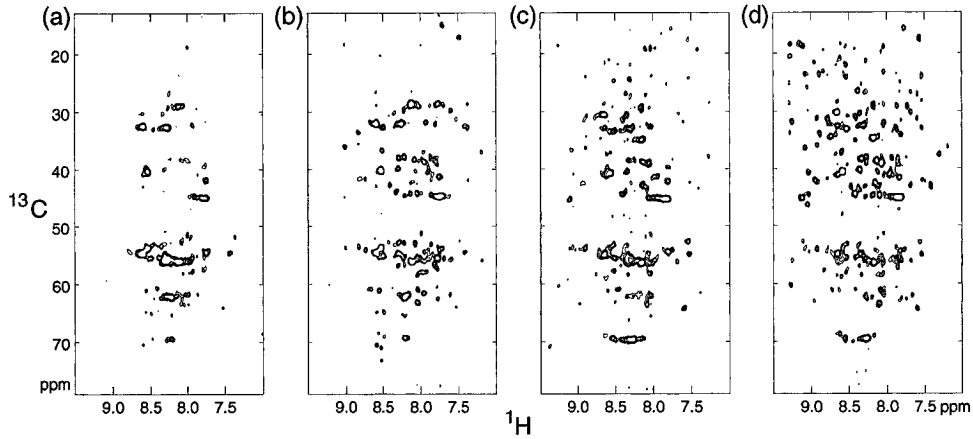

Figure 7. Two-dimensional $^{1}H_N-^{13}C$ spectra recorded using, in the case of spectra a and b, the 4D HBCB/HACA(CO)NNH and, in the case of spectra c and d, the 4D HCC(CO)NNH pulse sequence. Spectra a and b were recorded at 287 K (equivalent to a correlation time of 18 ns) on the fully protonated and 50% deuterated samples, respectively. Spectra c and d were recorded at 297 K (equivalent to a correlation time of 12 ns) on the fully protonated and 50% deuterated samples, respectively.

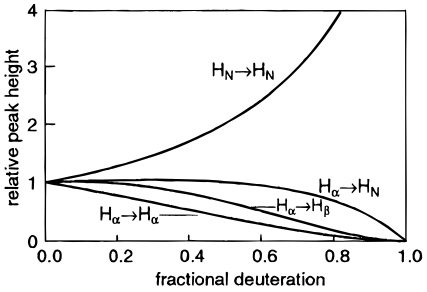

Figure 8. Simulations showing the relative peak height, as a function of deuteration level, expected for different kinds of cross peaks in 3D separated NOESY spectra; see text for the method of calculation. The intensities of the H_N-H_N and $H_\alpha-H_N$ cross peaks are computed for a 3D ^{15}N-separated NOESY, and those for the $H_\alpha-H_\alpha$ and $H_\alpha-H_\beta$ cross peaks are computed for a 3D ^{13}C-separated NOESY; the H_β are assumed to be part of a CH_2 group.

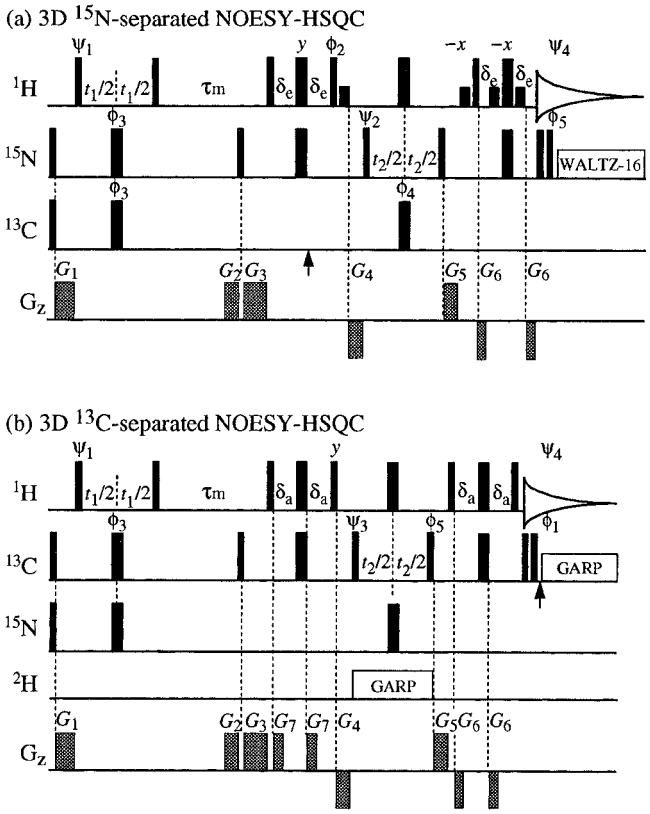

Figure 9. Pulse sequences for the 3D ^{15}N-separated NOESY-HSQC (a) and 3D ^{13}C-separated NOESY-HSQC (b). Except where mentioned below, details are as for the caption to Figure 3. ^{13}C RF pulses were applied with field strengths of 16.2 kHz, except during the periods of GARP decoupling where the RF field strength was reduced to 3.9 kHz. In each experiment the ^{13}C carrier was initially set to 43 ppm and switched to either 115.5 ppm (^{15}N-separated experiment) or 70 ppm (^{13}C-separated experiment) where indicated by arrows. Gradient pulses were applied with durations and strengths as follows: $G_1 = 5$ ms (40 G cm^{-1}); $G_2 = 2.0$ ms (40 G cm^{-1}); $G_3 = 4.0$ ms (35 G cm^{-1}); $G_4 = 2.5$ ms (30 G cm^{-1}); $G_5 = 1.0$ ms (30 G cm^{-1}); $G_6 = 0.4$ ms (30 G cm^{-1}); and $G_7 = 0.4$ ms (25 G cm^{-1}). The following phase cycling was employed: $\phi_1 = x, -x$; $\phi_2 = 4(y), 4(-y)$; $\phi_3 = -y, y$; $\phi_4 = 2(x), 2(-x)$; $\phi_5 = 4(x), 4(-x)$; $\psi_1 = x, -x$; $\psi_2 = \psi_3 = 2(x), 2(-x)$; $\psi_4 = x, -x, -x, x, -x, x, x, -x$. In the ^{15}N-separated experiment 45° is subtracted from the phase ψ_1. Quadrature detection is achieved by altering ψ_1, ψ_2 and ψ_3 in a States-TPPI, States-TPPI, and States manner,[40] respectively, to shift the axial peaks in the ^{1}H and ^{15}N dimensions to the edge of the spectrum.

effect dominates. Cross peaks between two H_α protons simply fall in intensity as the level of deuteration increases. This is attributed simply to the reduction in the number of protons; any advantage gained by the increase in the relaxation times of the

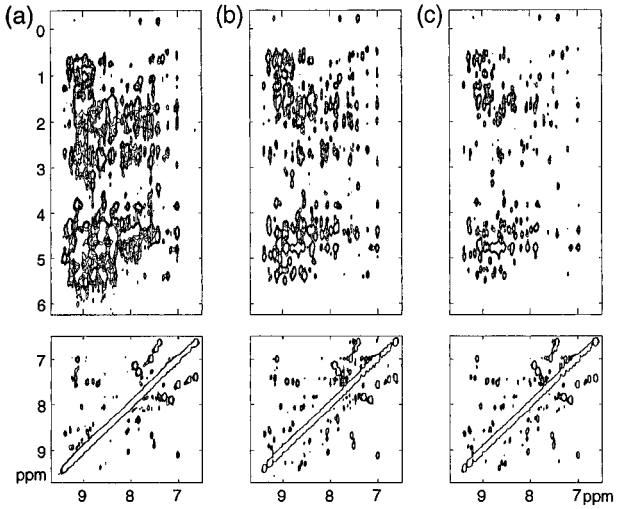

Figure 10. Two-dimensional ^{1}H$-^1H_N$ NOESY spectra recorded using the 3D ^{15}N-separated NOESY-HSQC pulse sequence of Figure 9a at 297 K (equivalent to a correlation time of 12 ns). In parts a, b, and c, the spectra of the fully protonated, the 50% deuterated, and the 75% deuterated samples, respectively, are shown.

H_α protons as the level of deuteration increases is outweighed by this dilution factor. Note, however, that the cross peaks are more intense than is predicted by the simple statistical factor, $(1 - \alpha)^2$. The cross-peak intensity between H_α and H_β does not fall as quickly as that for the $H_\alpha-H_\alpha$ cross peaks. This can be rationalized by noting that fragments **I** and **II** both contribute to the intensity of these cross peaks and that in fragment **II**, in which one H_β has been replaced by deuterium, the remaining H_β relaxes more slowly and hence gives a stronger peak. (In the context of the present discussion the C_α and C_β carbons shown in the fragments I−IV need not be located in the same residue.) In addition, the C_β relaxes more slowly in fragment **II** than it does in fragment **I**, a factor which favors moderate levels of deuteration.

Figure 10 compares two-dimensional ^{1}H$-^1$H NOESY spectra, recorded using the three-dimensional ^{15}N-separated NOESY pulse sequence[31] of Figure 9a, for the fully protonated, the 50% deuterated, and the 75% deuterated samples at a correlation time of 12 ns. As expected, the cross peaks between H_N protons increase in intensity as the level of deuteration increases. The cross peaks between H_N and H_α/H_β show comparable intensities for the fully protonated and 50% deuterated samples; indeed some are stronger in the spectrum from the latter sample. As predicted, increasing the level of deuteration to 75% reduces the intensity of these cross peaks. These spectra also show that as the level of deuteration increases there is a reduction in the line widths of the $H_{\alpha/\beta}-H_N$ cross peaks significantly improving the resolution; since the relaxation times of H_N increase more markedly with deuteration than do those of $H_{\alpha/\beta}$ the narrowing in the observed dimension is greater than that in the indirect dimension.

We have also compared two-dimensional ^{1}H$-^1$H NOESY spectra, recorded using the three-dimensional ^{13}C-separated NOESY pulse sequence[32,33] of Figure 9b, for the protonated and the 50% deuterated samples at a correlation time of 12 ns (data not shown). Some peaks are similar in intensity in the two spectra but on average the peaks in the spectrum from the deuterated sample are 0.5 times the intensity of those in the spectrum from the fully protonated sample; despite this reduction in intensity, the number of peaks visible in the two spectra are

(32) Ikura, M.; Kay, L. E.; Tschudin, R.; Bax, A. *J. Magn. Reson.* **1990**, *86*, 204−209.
(33) Zuiderweg, E. R. P.; McIntosh, L. P.; Dahlquist, F. W.; Fesik, S. W. *J. Magn. Reson.* **1990**, *86*, 210−216.

comparable. In the absence of relaxation effects the cross peaks from the 50% deuterated samples would be 0.25 times the intensity of those from the fully protonated sample. It is clear, therefore, that the more favorable relaxation of the deuterated protein is having a substantial effect on the intensity of these peaks. In a complete three-dimensional experiment, this comparison will improve further in favor of the deuterated protein due to slower ^{13}C relaxation in $^{13}CH_n$ groups (where $n \geq 2$).

It should be emphasized that in practice we expect that deuteration will not cause the intensity of the cross peaks to $H_{\alpha/\beta}$ to fall off as quickly as predicted by the plot in Figure 8. This is because of the influence that deuteration will have on the buildup curve for the NOE; as the level of deuteration increases there is less spin diffusion and so the maximum of the NOE buildup curve is greater and occurs at longer mixing times. We have so far compared ^{15}N- and ^{13}C-separated NOESY spectra recorded using a single mixing time of 50 ms, found to give the strongest $H_N-H_{\alpha/\beta}$ cross peaks in the spectrum from the fully protonated sample at a correlation time of 12 ns. It is expected that longer mixing times will increase the intensity of the cross peaks from the deuterated samples making their spectra compare more favorably with those from the fully protonated sample. In addition, when compared to the experimental results given above, the sensitivity of the $^{13}C/^{15}N$- and $^{13}C/^{13}C$-separated four-dimensional spectra[34−36] will improve due to the more favorable ^{13}C relaxation in $^{13}CH_n$ groups (where $n \geq 2$).

Conclusions

Our results show that a deuteration level of around 50% optimizes the sensitivity of experiments used to assign sidechain ^1H and ^{13}C resonances by correlating them with the resonances from backbone nuclei. We have also shown that in separated NOESY experiments the intensity of different kinds of cross peaks is optimized by different levels of deuteration. Although the observation of NOE contacts between aliphatic protons is best done using a fully protonated sample, a 50% deuterated sample is a good compromise for observing NOE contacts, in particular those involving H_N protons.

When it comes to assigning the backbone resonances, the experiments which are affected by deuteration can, for the purposes of the present discussion, be divided into two categories. The first category is typified by the HNCA experiment.[37] In this type of experiment the magnetization is transferred to C_α but not to H_α and so complete deuteration gives the largest sensitivity gain as a result of the much longer relaxation time of $C_\alpha D$. The second category of experiments is typified by the HNCAHA experiment.[38,39] In this type of experiment magnetization is derived from, or transferred to, H_α and, as has been described above, deuteration at any level simply dilutes away the H_α protons and so reduces the intensity of the resulting peaks.

A sample with 50% deuteration, chosen to maximize the signal intensity from the side-chain experiments, is not the optimum for either category of backbone experiments. However, compared to a fully protonated sample, a 50% deuterated sample will offer a very significant improvement in sensitivity for experiments in the first category. For experiments in the second category there will be a reduction in sensitivity. However, we would argue that, as these backbone experiments are in any case much more sensitive than those used to assign sidechain nuclei, some reduction in sensitivity from the optimum will be tolerable.

In the experiments we describe the resolution in the ^{13}C dimensions is insufficient to resolve peaks from different isotopomers. However, the observed peak positions will change with deuteration level as the intensities of the different unresolved contributions to the line shape vary. An advantage of using a single partially deuterated sample, labeled at 50% in order to optimize the sidechain experiments, for *all* experiments is that these isotope shifts will be the same in all spectra and so can be ignored (this assumes that all spectra have the same resolution in the ^{13}C dimensions).

In conclusion we have shown, both theoretically and experimentally, that the use of a ∼50% deuterated sample increases the sensitivity of experiments used to assign sidechain nuclei. For proteins with long correlation times (∼20 ns) this increase in sensitivity is by a factor of between 1.5 and 2.5. Of all the experiments used to determine protein structures these sidechain experiments are the first to fail as the size of the protein increases. Our aim, therefore, was to optimize the level of deuteration for these experiments in the expectation that a reduction in sensitivity in the more sensitive backbone and ^{13}C-separated NOESY experiments can be tolerated. The use of fractional deuteration should extend the upper limit on the maximum size of protein whose structure can be studied using this approach.

Acknowledgment. This work was supported by grants from the Science and Engineering Research Council and from the Biotechnology and Biological Sciences Research Council (BBSRC) of the UK. The Cambridge Centre for Molecular Recognition is supported by the BBSRC and the Wellcome Trust. H.O. and J.K. acknowledge support for a EUREKA project from the Bundesministerium für Bildung, Technologie und Forschung (Grant No. BEO11/17620A). We thank Dr. Detlef Moskau (Spectrospin AG, Fällanden, Switzerland) for the loan of probe heads and a gradient amplifier. D.N. thanks the Swiss National Science Foundation for a postdoctoral research fellowship. Y.I. thanks the Biodesign Research Programme (RIKEN) for financial support. We thank Dr. Brian Smith for help in preparing the samples, Mr. Rolf Tschudin (NIH, Bethesda, Maryland) for help with the modifications of our spectrometer for ^2H decoupling, and Dr. Sharon Archer for helpful comments on the manuscript.

Note Added in Proof: Recently Venters et. al. (Venters, R. A.; Metzler, W. J.; Spicer, L. D.; Mueller, L.; Farmer, B. T., II *J. Am. Chem. Soc.* **1995**, *117*, 9592−9593) and Grzesiek et al. (Grzesiek, S.; Wingfield, P.; Stahl, S.; Kaufman, J. D.; Bax, A. *J. Am. Chem. Soc.* **1995**, *117*, 9594−9595) have also demonstrated that high levels of deuteration are useful for the observation of NOE contacts between H_N protons in larger proteins.

JA952207B

(34) Kay, L. E.; Clore, G. M.; Bax, A.; Gronenborn, A. M. *Science* **1990**, *249*, 411−414.
(35) Clore, G. M.; Kay, L. E.; Bax, A.; Gronenborn, A. M. *Biochemistry* **1991**, *30*, 12−18.
(36) Zuiderweg, E. R. P.; Petros, A. M.; Fesik, S. W.; Olejniczak, E. T. *J. Am. Chem. Soc.* **1991**, *113*, 370−372.
(37) Kay, L. E.; Ikura, M.; Tschudin, R.; Bax, A. *J. Magn. Reson.* **1990**, *89*, 496−514.
(38) Kay, L. E.; Wittekind, M.; McCoy, M. A.; Friedrichs, M. S.; Mueller, L. *J. Magn. Reson.* **1992**, *98*, 443−450.
(39) Clubb, R. T.; Thanabal, V.; Wagner, G. *J. Bimol. NMR* **1992**, *2*, 203−210.
(40) Marion, D.; Ikura, M.; Tschudin, R.; Bax, A. *J. Magn. Reson.* **1989**, *85*, 393−399.
(41) Kay, L. E.; Xu, G. Y.; Yamazaki, T. *J. Magn. Reson. A* **1994**, *109*, 129−133.
(42) Grzesiek, S.; Bax, A. *J. Am. Chem. Soc.* **1993**, *115*, 12593−12594.
(43) Stonehouse, J.; Clowes, R. T.; Shaw, G. L.; Keeler, J.; Laue, E. D. *J. Biomol. NMR* **1995**, *5*, 226−232.
(44) Stonehouse, J.; Shaw, G. L.; Keeler, J.; Laue, E. D. *J. Magn. Reson. A* **1994**, *A107*, 178−184.